

- [5] M. Driess, H. Pritzkow, S. Rell, unpublished results. Compound **6** is formed by salt condensation from  $\text{Is}(\text{tBu})\text{Si}(\text{F})\text{-PHLi}$  with  $\text{Is}(\text{tBu})\text{SiFCl}$ .  $\text{Is} = 2,4,6\text{-iPr}_3\text{C}_6\text{H}_2$ .
- [6] Crystal structure analyses: All intensity measurements were carried out on a Siemens-Stoe AED2 diffractometer at  $-70^\circ\text{C}$ . The H atoms were placed in calculated positions, and the other atoms refined anisotropically [15]. **7**: rhombic, space group  $P2_12_12_1$ ,  $a = 15.392(8)$ ,  $b = 17.995(9)$ ,  $c = 18.026(9)$  Å,  $V = 4993$  Å<sup>3</sup>,  $Z = 4$ , 4880 independent reflections ( $\text{MoK}\alpha$  radiation,  $\omega$  scans,  $2\theta_{\text{max}} = 50$ ),  $R1 = 0.047$  (observed reflections,  $I > 2\sigma(I)$ ),  $wR2 = 0.126$  (all reflections) [15b]. The THF molecules are disordered. **1**: monoclinic, space group  $C2/c$ ,  $a = 27.94(2)$ ,  $b = 9.905(6)$ ,  $c = 21.443(14)$  Å,  $\beta = 138.34(3)^\circ$ ,  $V = 3945$  Å<sup>3</sup>,  $Z = 4$ , 3883 independent reflections ( $\text{MoK}\alpha$  radiation,  $\omega$  scans,  $2\theta_{\text{max}} = 54$ ).  $R1 = 0.063$  (observed reflections,  $I > 2\sigma(I)$ ),  $wR2 = 0.169$  (all reflections) [15b]. The molecule is disordered; two sites are half occupied by a phosphorus and fluorine atom, respectively. Moreover, the *tert*-butyl groups and the aryl substituents show rotational disorder. **3**: triclinic, space group  $P1$ ,  $a = 9.312(8)$ ,  $b = 10.300(8)$ ,  $c = 11.673(9)$  Å,  $\alpha = 74.35(6)$ ,  $\beta = 78.38(6)$ ,  $\gamma = 65.63(6)$ ,  $V = 976.8$  Å<sup>3</sup>,  $Z = 1$ , 5591 independent reflections ( $\text{MoK}\alpha$  radiation,  $\omega$  scans,  $2\theta_{\text{max}} = 60$ ),  $R1 = 0.056$  (observed reflections,  $I > 2\sigma(I)$ ),  $wR2 = 0.137$  (all reflections) [15b]. The crystals contain about 14 % of **8** as an impurity. The observed structure is an overlap of both structures. Crystallographic data (excluding structure factors) for the structures reported in this paper have been deposited with the Cambridge Crystallographic Data Centre as supplementary publication no. CCDC-100141. Copies of the data can be obtained free of charge on application to The Director, CCDC, 12 Union Road, Cambridge CB21EZ, UK (fax: int. code + (1223) 336-033; e-mail: deposit@chemcrs.cam.ac.uk).
- [7] U. Klingebiel, M. Meyer, U. Pieper, D. Stalke, *J. Organomet. Chem.* **1991**, *408*, 19.
- [8] M. Driess, U. Winkler, W. Imhof, L. Zsolnai, G. Huttner, *Chem. Ber.* **1994**, *127*, 1031, and references therein.
- [9] GAUSSIAN 94, Revision B.3., M. J. Frisch, G. W. Trucks, H. B. Schlegel, P. M. W. Gill, B. G. Johnson, M. A. Robb, J. R. Cheeseman, T. Keith, G. A. Petersson, J. A. Montgomery, K. Raghavachari, M. A. Al-Laham, V. G. Zakrzewski, J. V. Ortiz, J. B. Foresman, C. Y. Peng, P. Y. Ayala, W. Chen, M. W. Wong, J. L. Andres, E. S. Replogle, R. Gomperts, R. L. Martin, D. J. Fox, J. S. Binkley, D. J. Defrees, J. Baker, J. P. Stewart, M. Head-Gordon, C. Gonzalez, J. A. Pople, Gaussian, Inc., Pittsburgh PA, **1995**.
- [10] N. Wiberg, H. Köpf, *Chem. Ber.* **1987**, *120*, 653.
- [11] M. Driess, H. Pritzkow, *Z. Anorg. Allg. Chem.* **1996**, *622*, 858.
- [12] W. W. Schoeller, T. Busch, *J. Chem. Soc. Chem. Commun.* **1989**, 234.
- [13] M. Baudler, H. Jongebloed, *Z. Anorg. Allg. Chem.* **1979**, *458*, 9; M. Weidenbruch, M. Herrndorf, A. Schaefer, K. Peters, H. G. von Schnering, *J. Organomet. Chem.* **1985**, *295*, 7; M. Baudler, T. Pontzen, *Z. Anorg. Allg. Chem.* **1982**, *491*, 27; M. Driess, H. Pritzkow, *Angew. Chem.* **1992**, *104*, 775; *Angew. Chem. Int. Ed. Engl.* **1992**, *31*, 751; M. Driess, H. Pritzkow, M. Reising, *Chem. Ber.* **1991**, *124*, 1923.
- [14] Recent review on  $\text{Si}_2\text{X}$  three-membered rings: M. Weidenbruch, *Chem. Rev.* **1995**, *95*, 1489, and references therein.
- [15] a) G. M. Sheldrick, *SHELXS86*, Universität Göttingen (Germany), **1986**;  
b) G. M. Sheldrick, *SHELXL93*, Universität Göttingen, **1993**.

## Hexaphenylethane Derivatives Exhibiting Novel Electrochromic Behavior\*\*

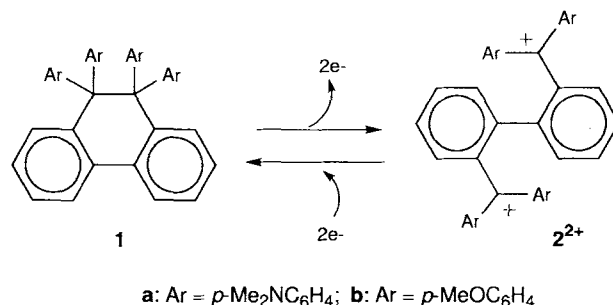
Takanori Suzuki,\* Jun-ich Nishida, and Takashi Tsuji

9,9,10,10-Tetraphenyl-9,10-dihydrophenanthrene (**3**) is a stable molecule<sup>[1]</sup> whose central C–C bond is predicted to be the longest among “clamped” hexaphenylethane derivatives.<sup>[2]</sup> Although this weakened bond is resistant to homolytic rupture,

[\*] Prof. T. Suzuki, J. Nishida, Prof. T. Tsuji  
Division of Chemistry, Graduate School of Science  
Hokkaido University, Sapporo 060 (Japan)  
Fax: Int. code + (11) 746-2557  
e-mail: tak@science.hokudai.ac.jp

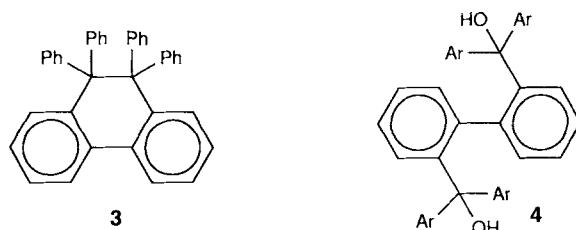
[\*\*] This work was supported by the Ministry of Education, Science, and Culture of Japan (Grant No. 06640675 and 08640664) and by Hokscitec Foundation. We thank Prof. Tamotsu Inabe (Hokkaido University) for the use of facilities to analyze the X-ray structures.

the activation energy for its scission can be lowered by electron transfer,<sup>[3]</sup> especially when suitable substituents are introduced. Bearing this in mind, we have now designed a new redox system in which reversible C–C bond breaking and bond making occur upon two-electron transfer (Scheme 1). This system has the fol-



Scheme 1. Dynamic redox behavior of **1** and  $2^{2+}$ .

lowing interesting features: 1) the four dimethylamino and methoxy substituents in **1a** and **1b**, respectively, should facilitate the removal of electrons from these molecules, thereby activating the scissile bond; 2) the central bond in **1** like that in **3** is still expected to be sufficiently stable against homolysis taking into consideration that the aromatic substituents have little effect on the Gibbs activation energy of the homolytic cleavage  $\Delta G_{\text{homolysis}}^\ddagger$  in 1,2-diarylethanes;<sup>[3,4]</sup> 3) the dications  $2^{2+}$  formed by the oxidation of **1** should be stabilized by delocalization of each positive charge over half of the molecule and due to the presence of the triarylmethylenium chromophores these cations are intensely colored; 4) the interconversions between **1** and  $2^{2+}$  should proceed very cleanly because they are intramolecular processes. Here we report the preparation, properties, and structures of these novel redox couples.



The dication salts  $2\mathbf{a}^{2+}(\text{BF}_4^-)_2$  and  $2\mathbf{b}^{2+}(\text{BF}_4^-)_2$  were obtained in 98 and 93% yield by treating the diols **4a**<sup>[5]</sup> and **4b**, respectively, with  $\text{HBF}_4$ . Reduction of these salts with Mg in MeCN gave ethanes **1a** and **1b** as stable solids in 86 and 93% yield, respectively. On the other hand, oxidation of **1a** and **1b** with two equivalents of  $(p\text{-BrC}_6\text{H}_4)_3\text{N}^+\text{SbCl}_6^-$  in  $\text{CH}_2\text{Cl}_2$  led to the regeneration of the dications  $2\mathbf{a}^{2+}$  and  $2\mathbf{b}^{2+}$ , which were isolated as  $\text{SbCl}_6^-$  salts in 85 and 97% yield, respectively. The high-yield interconversions between **1** and  $2^{2+}$  indicate that they constitute “reversible” redox couples, although the bond breaking and making are induced by electron transfer.

The sharp contrast in the UV/Vis spectra of these couples is noteworthy. Ethanes **1** show absorption only in the UV region, whereas intense absorption bands in the visible region occur for the dications  $2\mathbf{a}^{2+}$  [ $\lambda_{\text{max}}$  (MeCN): 661 (lgε 4.92), 604 nm (5.05)] and  $2\mathbf{b}^{2+}$  [539 sh (4.72), 514 (4.87)]. Thus, electrochromic systems with color changes from colorless to deep blue and colorless to deep red could be constructed by using *p*-dimethylamino

and *p*-methoxy derivatives, respectively. Spectrophotometric monitoring of the electrochemical reduction of  $2^{2+}$  to **1** revealed the presence of several isosbestic points in both cases (Figure 1), indicating the quantitative conversion as well as the negligible steady-state concentration of the intermediary cation radicals.

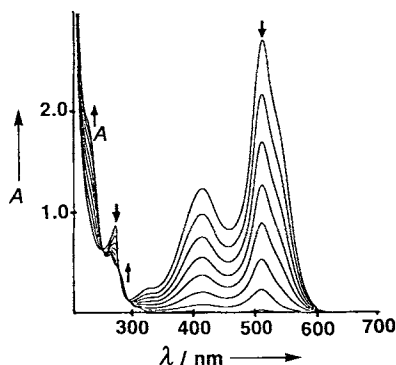


Figure 1. Change in UV/Vis spectrum of  $2b^{2+}(BF_4^-)_2$  ( $3.6 \times 10^{-5}$  mol dm $^{-3}$ , 2 mL) upon electrochemical reduction (10  $\mu$ A) at 3 min intervals. The coulometric analysis indicates that the interconversion is a two-electron process.

Not only the color but also the geometry change drastically during the interconversion, as determined by the X-ray structure analyses.<sup>[6]</sup> While the biphenyl skeleton of **1b** is nearly planar (Figure 2a), the two molecular halves in  $2a^{2+}$  are twisted by 69° around the biphenyl axis; the distance between the two methylenium carbon atoms is 3.66(2) Å (Figure 2b). Such a dy-

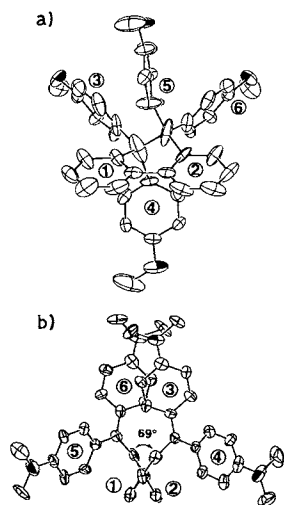


Figure 2. a) Molecular geometry of **1b** determined by X-ray structure analysis on the **1b**·THF solvate crystal. Two aryl groups (3 and 6) are equatorial and the other two (4 and 5) are axial substituents in the pseudo-half-chair six-membered ring. b) Molecular geometry of  $2a^{2+}$  determined by X-ray structure analysis on the  $2a^{2+}(SbCl_6^-)_2$  salt. The dication has pseudo- $C_2$  symmetry. Two aryl groups (3 and 6) overlap each other in a face-to-face manner (interplanar distance, 3.37 Å; dihedral angle 11.5°), indicating the  $\pi$ - $\pi$  interaction between these rings.

namic change in structure causes the hysteretic redox properties of **1** and  $2^{2+}$  (Figure 3). Thus, **1a** and **1b** undergo electrochemical oxidation at peak potentials of +0.77 and +1.47 V vs. SCE in  $CH_2Cl_2$ , respectively. These processes are irreversible in the sense that the corresponding cathodic peaks were absent in the cyclic voltammograms (scan rate: 100–500 mV s $^{-1}$ ). Instead, new peaks appeared in the far cathodic region (–0.45 and +0.18 V, respectively), which were assigned to the reduction potentials of  $2a^{2+}$  and  $2b^{2+}$ . This assignment was confirmed by separate measurements on  $2^{2+}(BF_4^-)_2$  salts under the same conditions. Again, quite similar hysteretic behavior was observed in the voltammograms of  $2^{2+}$ , which showed new anodic peaks corresponding to the oxidation potentials of **1**.

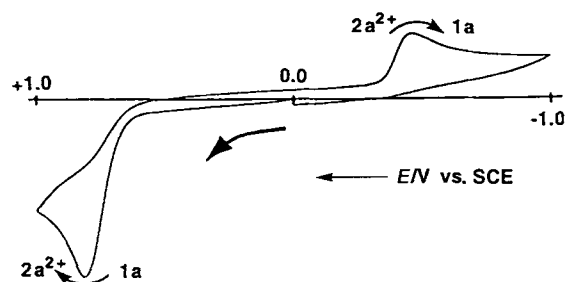


Figure 3. Cyclic voltammogram of **1a** in  $CH_2Cl_2$  (0.1 M  $nBu_4NBF_4$ , Pt electrode, scan rate 500 mV s $^{-1}$ ). The reduction peak at –0.45 V was absent when the voltammogram was first scanned to the cathode.

Such separation of redox potentials is characteristic of “dynamic redox systems” that undergo reversible and drastic structural change during electron transfer, as in the present case.<sup>[7]</sup> In the region between the reduction potential and the oxidation potential, both the reduced form (**1**) and the oxidized form ( $2^{2+}$ ) can coexist in any ratio. By combining **1** with a suitable electron acceptor, it may be possible to apply this unique feature to the construction of novel redox-type photochromic systems in which the back reactions in the dark become endothermic due to the large shift of redox potentials.

#### Experimental Section

**4b**: The reaction of 4,4'-dimethoxybenzophenone and 2,2'-dilithiobiphenyl in THF afforded **4b** as a colorless powder in 47% yield. M.p. 226–228 °C;  $^1H$  NMR (90 MHz,  $CDCl_3$ ):  $\delta$  = 6.97–7.13 (m, 10H), 6.71–6.89 (m, 12H), 6.05–6.15 (m, 2H), 4.35 (s, 2H), 3.82 (s, 6H), 3.78 (s, 6H).

$2^{2+}(BF_4^-)_2$ : To a solution of diol **4a** (5.65 g, 8.18 mmol) in THF (100 mL) was added 42%  $HBF_4$  (2.60 mL, 17.4 mmol) over 10 min at 0 °C. After the mixture had been stirred for 18 h at room temperature, deep-blue microcrystals of  $2a^{2+}(BF_4^-)_2$  (6.64 g, 98%) were filtered, and washed with THF and ether, m.p. 316–317 °C (decomp);  $^1H$  NMR (400 MHz,  $CDCl_3$ , 25 °C):  $\delta$  = 7.60 (br., 2H), 7.23 (ddd,  $J$  = 7.6, 7.6, 1.5 Hz, 2H), 7.17 (ddd,  $J$  = 7.6, 7.6, 1.5 Hz, 2H), 7.13 (br. AA'XX', 4H), 7.05 (dd,  $J$  = 7.6, 1.5 Hz, 2H), 6.98 (dd,  $J$  = 7.6, 1.5 Hz, 2H), 6.92–7.02 (br., 6H), 6.77 (br. AA'XX', 4H), 3.37 (s, 12H), 3.20 (s, 12H);  $^{13}C$  NMR (100 MHz,  $CD_3CN$ ):  $\delta$  = 174.65, 158.21, 157.26, 143.86, 141.99, 140.38, 139.67, 133.93, 133.61, 131.29, 128.16, 128.04, 127.85, 114.81, 114.08, 41.50, 41.04; UV/Vis (MeCN):  $\lambda_{max}$  (lge) = 661 (4.92), 604 (5.05), 431 (4.50), 408 (4.41), 319 nm (4.50). Diol **4b** was similarly treated with 42%  $HBF_4$  in propionic anhydride, and  $2b^{2+}(BF_4^-)_2$  was obtained as a red powder in 93% yield, m.p. 200.5–202 °C (decomp);  $^{13}C$  NMR (100 MHz,  $CD_3CN$ ):  $\delta$  = 192.63, 175.39, 172.50, 146.8 (br.), 144.39, 143.02, 140.93, 136.63, 134.48, 134.42, 134.04, 132.56, 128.62, 118.47, 117.71, 59.09, 58.20; UV/Vis (MeCN):  $\lambda_{max}$  (lge) = 539 sh (4.72), 514 (4.87), 416 (4.54), 335 (3.83), 274 nm (4.36).

**1**: A suspension of  $2b^{2+}(BF_4^-)_2$  (173 mg, 0.222 mmol) and Mg turnings (740 mg, 30.4 mmol) in dry MeCN (10 mL) was stirred for 22 h at room temperature. The solvent was evaporated, and the residue was triturated with benzene. Chromatographic separation on  $Al_2O_3$  (benzene) afforded **1b** (126 mg, 93%) as a colorless solid, m.p. 270–272 °C (decomp);  $^1H$  NMR (400 MHz,  $CDCl_3$ , 50 °C):  $\delta$  = 7.68 (dd,  $J$  = 7.8, 1.5 Hz, 2H), 7.23 (ddd,  $J$  = 7.8, 7.8, 1.5 Hz, 2H), 7.16 (dd,  $J$  = 7.8, 1.5 Hz, 2H), 7.11 (ddd,  $J$  = 7.8, 7.8, 1.5 Hz, 2H), 6.93 (br., 8H), 6.48 (br., 8H), 3.70 (s, 12H); UV/Vis (MeCN):  $\lambda_{max}$  (lge) = 287 (4.13), 274 nm (4.25). Similarly **1a** was obtained as a colorless solid in 86% yield by Mg reduction of  $2a^{2+}(BF_4^-)_2$ , m.p. 315–317 °C (decomp);  $^1H$  NMR (400 MHz,  $CDCl_3$ , 50 °C):  $\delta$  = 7.65 (dd,  $J$  = 7.8, 1.0 Hz, 2H), 7.21 (dd,  $J$  = 7.8, 1.0 Hz, 2H), 7.18 (ddd,  $J$  = 7.8, 7.8, 1.0 Hz, 2H), 7.07 (ddd,  $J$  = 7.8, 7.8, 1.0 Hz, 2H), 6.91 (br. AA'XX', 8H), 6.31 (br. AA'XX', 8H), 2.83 (s, 24H); UV/Vis (MeCN):  $\lambda_{max}$  (lge) = 268 nm (4.87).

$2^{2+}(SbCl_6^-)_2$ : To a solution of **1a** (35 mg, 0.053 mmol) in  $CH_2Cl_2$  (10 mL) was added (*p*-BrC $_6$ H $_4$ ) $_2$ N $^+$ SbCl $_6^-$  (90 mg, 0.110 mmol), and the mixture was stirred for 1.5 h at room temperature. Deep blue precipitates of  $2a^{2+}(SbCl_6^-)_2$  (60 mg, 85%) were filtered, and washed with  $CH_2Cl_2$ , m.p. 300–320 °C (decomp). Similar oxidation of **1b** afforded  $2b^{2+}(SbCl_6^-)_2$  in 97% yield, m.p. 174.5–177 °C (decomp);  $^1H$  NMR (400 MHz,  $CD_3CN$ , 24 °C):  $\delta$  = 7.46 (ddd,  $J$  = 7.3, 7.3, 1.5 Hz, 2H), 7.41 (ddd,  $J$  = 7.3, 7.3, 1.5 Hz, 2H), 7.33 (dd,  $J$  = 7.3, 1.5 Hz, 2H), 7.23–7.33 (br. AA'XX', 8H), 7.17 (dd,  $J$  = 7.3, 1.5 Hz, 2H), 7.09–7.15 (br. AA'XX', 8H), 4.09 (br. s, 6H), 4.07 (br. s, 6H).

All the new compounds gave satisfactory analytical data, and IR and mass spectra.

Received: November 4, 1996 [Z97261E]  
German version: *Angew. Chem.* 1997, 109, 1387–1389

**Keywords:** carbocations · dyes · electrochemistry · redox chemistry

- [1] G. Wittig, H. Petri, *Justus Liebig's Ann. Chem.* **1933**, 505, 17.  
 [2] W. D. Hounshell, D. A. Dougherty, J. P. Hummel, K. Mislou, *J. Am. Chem. Soc.* **1977**, 99, 1916.  
 [3] P. Maslak, J. N. Narvaez, T. M. Vallombroso, Jr., *J. Am. Chem. Soc.*, **1995** 117, 12373; P. Maslak, W. H. Chapman, Jr., T. M. Vallombroso, Jr., B. A. Watson, *ibid.* **1995**, 117, 12380.  
 [4] G. Kratt, H. -D. Beckhaus, C. Ruchardt, *Chem. Ber.* **1984**, 117, 1748.  
 [5] G. Wittig, W. Herwig, *Chem. Ber.* **1954**, 87, 1511.  
 [6] **1b**·THF:  $C_{42}H_{36}O_4 \cdot C_4H_8O$ , orthorhombic  $Pna2_1$ ,  $a = 8.277(2)$ ,  $b = 34.15(1)$ ,  $c = 13.025(5)$  Å,  $V = 3681(2)$  Å<sup>3</sup>,  $\rho_{\text{calcd}}$  ( $Z = 4$ ) = 1.222 g cm<sup>-3</sup>,  $R = 0.086$ . The structural parameters of **1b** are not reliable enough to allow a comparison with those of calculated **3** due to the low quality of the data for the structural determination (large thermal motion and positional disorder). **2a**<sup>2+</sup>(SbCl<sub>6</sub><sup>-</sup>)<sub>2</sub> salt:  $C_{44}H_{44}Cl_{12}N_4Sb_2$ , monoclinic  $C2/c$ ,  $a = 34.187(6)$ ,  $b = 12.638(6)$ ,  $c = 30.664(6)$  Å,  $\beta = 119.98(1)^\circ$ ,  $V = 11475(6)$  Å<sup>3</sup>,  $\rho_{\text{calcd}}$  ( $Z = 8$ ) = 1.535 g cm<sup>-3</sup>,  $R = 0.079$ . Crystallographic data (excluding structure factors) for the structures reported in this paper have been deposited with the Cambridge Crystallographic Data Centre as supplementary publication no. CCDC-100006. Copies of the data can be obtained free of charge on application to The Director, CCDC, 12 Union Road, Cambridge CB2 1EZ, UK (fax: int. code + (1223) 336-033; e-mail deposit@chemcrs.cam.ac.uk).  
 [7] Similar potential separation was also observed in 1,3-dimethylenecyclobutanes or bicyclic trichalcogenides which undergo structural change accompanied with transannular bonding upon two-electron oxidation: M Horner, S. Hünig, *J. Am. Chem. Soc.* **1977**, 99, 6122; H. Fujihara, H. Mima, T. Erata, N. Furukawa, *ibid.* **1992**, 114, 3117. Linkage isomerism in the transition metal complexes also leads to molecular hysteresis of this kind: M. Sano, H. Taube, *ibid.* **1991**, 113, 2327; A. Livoreil, C. O. Dietrich-Buchecker, J. -P. Sauvage, *ibid.* **1994**, 116, 9399.

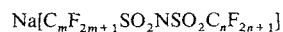
## Perfectly Staggered and Twisted Difluoromethylene Groups in Perfluoroalkyl Chains: Structure of $M[C_4F_9SO_2NSO_2C_4F_9]$ ( $M = Na, K$ )\*\*

Lixin Xue, Darryl D. DesMarteau,\* and William T. Pennington\*

In contrast to the perfectly all-staggered conformation observed for *n*-alkanes, the generally accepted structure of a perfluorinated *n*-alkane involves a helical conformation of the carbon backbone.<sup>[1]</sup> This is presumably due to the larger van der Waals radius of fluorine relative to that of hydrogen; rotation about the carbon-carbon chain bonds occurs to increase the distance between fluorine atoms on carbon atoms separated by one CF<sub>3</sub> group.<sup>[2]</sup>

Polytetrafluoroethylene possesses a helical structure at ambient conditions, but undergoes a solid-solid phase transition to a planar zigzag conformation under increased pressure.<sup>[3,4]</sup> A similar transition occurs for perfluoro-*n*-alkanes, but at considerably lower pressure.<sup>[5]</sup> In a recent article it has been suggested that short perfluorinated carbon chains take on a planar zigzag structure rather than a helical one at ambient pressure, when closely packed on the surface of a substrate.<sup>[6]</sup> In that report, the structures of thin films of perfluorodecanoic acid deposited on

glass were investigated by a combination of low-angle X-ray diffraction, X-ray grazing-incidence diffraction and molecular modeling. The compound was found to be present as two phases, and for both phases the best model had carbon chains that were untwisted. We have obtained more direct evidence, based on single-crystal X-ray diffraction analysis, of similar behavior for the perfluoro-*n*-alkyl side chains of the sodium salts **1–3** of bis[(perfluoroalkyl)sulfonyl] imides.



**1**,  $m = n = 4$ ; **2**,  $m = n = 6$ ; **3**,  $m = 4$ ,  $n = 6$

In this communication, we report the crystal structure of **1**,<sup>[7]</sup> a representative member of the series, and contrast its structure with that of a potassium derivative of **1** (compound **4**,  $m = n = 4$ ).<sup>[8]</sup> A more thorough discussion of all of these compounds will appear later.<sup>[9]</sup>

The remarkable acidity of bis[(perfluoroalkyl)sulfonyl] imides<sup>[10,11]</sup> is due, in part, to the resonance stabilization of the conjugate base anions of the acids. Extensive delocalization of charge over the SO<sub>2</sub>-N-SO<sub>2</sub> framework allows these anions to serve as multidentate ligands that bond to multiple metal centers to maximize electrostatic interaction.<sup>[12]</sup> These interactions result in the formation of ionic hydrophilic regions and perfluoro hydrophobic regions, which typically associate into layers consisting of an ionic core and perfluoro surfaces.<sup>[13,14]</sup> This behavior is observed in **1**; the sodium ion (Figure 1, left) interacts strongly with the nitrogen atom of the anion (interatomic distance 2.531(7) Å) and is chelated by a pair of sulfonyl oxygen atoms (Na1-O1b, O1c 2.331(5) Å) of an anion related by translation along the *b* axis to form ion-pair chains; chains related by inversion symmetry (1/2, 0, 0) are connected by additional interactions between the sodium ion and sulfonyl oxygen atoms (Na1-O2d, O2e 2.356(4) Å) to form layers, which stack along the *a* axis (Figure 1, right). Due to the strong interactions in-

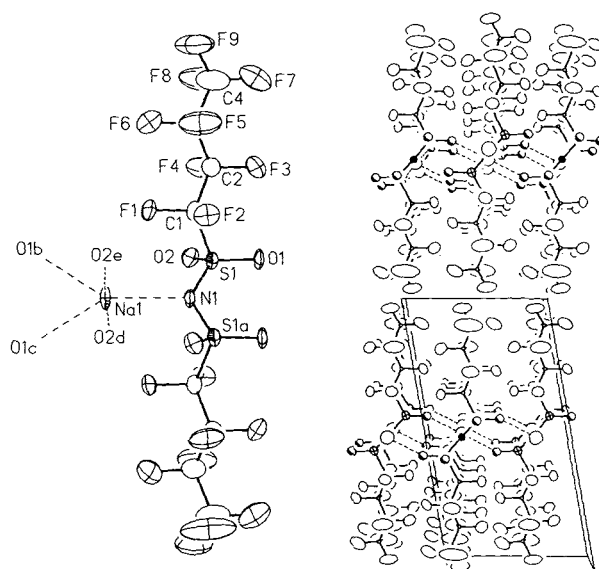


Figure 1. a) Left: Crystal structure of **1** (thermal ellipsoids at 50% probability), showing the interionic contacts and the atom labeling scheme used. Atoms containing a lower case character in their labels were generated by the following symmetry operations: a)  $1-x, y, 1/2-z$ ; b)  $x, y, -1, z$ ; c)  $1-x, y, -1, 1/2-z$ ; d)  $1-x, -y, -z$ ; e)  $x, -y, 1/2+z$ . Right: crystal packing of **1** viewed down the *b* axis. The origin is the lower left rear corner;  $+x$  is up,  $+y$  is out and  $+z$  is to the right. The sulfur atoms are represented as hatched ellipsoids, the sodium ions as large open circles, the fluorine atoms as boundary ellipsoids, the oxygen atoms as shaded circles, the nitrogen atoms as solid circles, and the carbon atoms as small open circles.

[\*] Dr. D. D. DesMarteau, Dr. W. T. Pennington, L. Xue  
 Department of Chemistry, Hunter Research Laboratory  
 Clemson University  
 Clemson, SC 29634-1905 (USA)  
 Fax: Int. code + (864) 656-6613  
 e-mail: bill.pennington@ces.clemson.edu

[\*\*] Support of this work by the National Science Foundation (CHE-9133028, CHE-9207230, and OSR-9108772) and the Department of Energy (Cooperative Agreement DE-FC02-91ER-75666, "DOE/EPSCoR Research Implementation Plan") is gratefully acknowledged.